# Radial Excitation of the Nucleon to the $P_{11}(1440\ \text{MeV})$ Resonance in Alpha-Proton Scattering

H. P. Morsch,[a] M. Boivin, W. Jacobs,[b] F. Plouin, W. Spang, J. Yonnet, and P. Zupranski[c]
*Laboratoire National Saturne, F-91191 Gif-sur-Yvette CEDEX, France*

R. Frascaria, R. Siebert, E. Warde, and J. P. Didelez
*Institut de Physique Nucléaire Orsay, F-91406 Orsay CEDEX, France*

B. Saghai
*Service de Physique Nucléaire, Centre d'Etudes Nucléaires de Saclay, F-91191 Gif-sur-Yvette CEDEX, France*

P. E. Tegnér
*Department of Physics, Stockholm University, S-11346 Stockholm, Sweden*
(Received 3 December 1991)

The energy region from the $\pi$ threshold up to the Roper resonance $N(1440)$ has been investigated in inelastic $\alpha$ scattering on hydrogen using $\alpha$ particles from SATURNE with a beam momentum of 7 GeV/$c$. In addition to projectile excitation, excitation of the $P_{11}(1440\ \text{MeV})$ resonance has been observed for the proton, indicating a strong monopole excitation. From this a value of the nucleon compressibility of $1.4 \pm 0.3$ GeV is extracted.

PACS numbers: 25.55.Ci, 14.20.Gk, 25.10.+s

The detailed experimental study of the baryon properties presents an exciting challenge in hadronic physics for the next decade since it is related to the understanding of the structure of QCD in the nonperturbative regime. For the description of the baryon properties different theoretical approaches [1–4] exist and are under development. These have to be tested in specific experiments using both electromagnetic and hadronic probes. One of the most basic degrees of freedom is the size of the baryon. Its static properties are given, e.g., by the charge densities studied in electron scattering. The different charge densities for protons and neutrons can be understood in models which give a baryon number density (with a radius much smaller than the nucleon radius) surrounded by a meson cloud [5]. Dynamical properties of the size degree of freedom can be studied in radial modes (isoscalar monopole excitations) which give information on the compressibility of the system. A candidate for a radial mode of the nucleon is the $P_{11}(1440\ \text{MeV})$ resonance.

The energy of the radial mode of excitation is critically dependent on the basic parameters of the different baryon models; e.g., it depends on the confining potential in the constituent quark model [2]. In bag models the radial mode depends on the bag size. Models have been proposed [6–8] in which the radial mode is generated by the oscillation of the bag surface. Skyrmion models [9] predict a radial mode which is rather low in energy.

The study of radial modes of excitations appears to be difficult because in proton-nucleon scattering the excitation spectrum is dominated by spin-isospin modes. Further, these particular modes are weakly excited by electromagnetic probes. Therefore, it is important to use selective probes which may enhance the cross sections. A favorable reaction appears to be the inelastic scattering by $\alpha$ particles because in the forward scattering scalar excitations (without spin and isospin flip, $S=I=0$) should be dominant due to the structure of the $\alpha$ particle (see also Ref. [10]).

In the investigation of this reaction there are complications due to the fact that both the target as well as the projectile can be excited. The two dominant graphs for the $\alpha+p \rightarrow \alpha'+X$ reaction at appropriate energies are given in Fig. 1. Graph 1 corresponds to $N^*$ excitation discussed above. Graph 2 corresponds to an excitation in the projectile. Since there are no selection rules which inhibit $\Delta$ excitation in the $\alpha$ particle, the largest contribution should be due to excitation of the $\Delta(1232\ \text{MeV})$ resonance. By emission of a pion this excitation decays favorably back into the $\alpha$-particle ground state observed

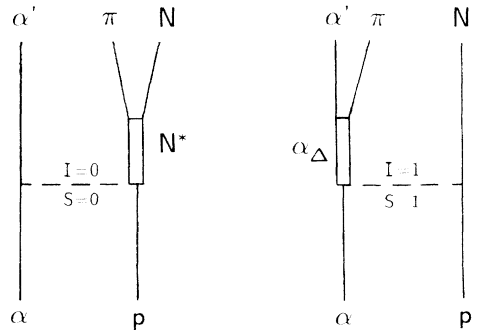


FIG. 1. Dominant graphs for target and projectile excitation, given by 1 and 2, respectively, which contribute to $\alpha+p \rightarrow \alpha'+X$ scattering.

in the detector. This process can explain almost quantitatively the old $\alpha+p$ scattering data [10], where a strong enhancement was observed above the $\pi$ threshold. To account for the yield of graph 2 in the inclusive $(\alpha,\alpha')$ spectra, calculations were performed within the impulse approximation using the meson-exchange model. Here, the parametrization by Ref. [11] has been used which describes quantitatively the cross sections and spectral shape of the elementary $pp \rightarrow n\Delta^{++}$ system. The matrix elements for the elementary $\Delta$-production processes with protons and neutrons were introduced into the Monte Carlo code FOWL and folded with the $\alpha$-particle form factor which describes elastic scattering. A ground-state branching $B(\alpha_\Delta \rightarrow \alpha_{g.s.}+\pi)$ of 0.2–0.3 was obtained by the normalization to the experimental data. It should be noted that a similar mechanism has been applied for $d+p$ scattering in Ref. [12]. The appearance of this contribution in the missing-mass spectra close to the pion threshold is due to the projectile velocity giving rise to a Lorentz boost in the energy spectra. Therefore, the spectral shape for this process is quite independent of the $\Delta$ resonance parameters. This is important for the analysis discussed below. Finally, it should be noted that in addition to the graphs in Fig. 1 there are other graphs giving rise to nonresonant contributions for target and projectile excitation. For projectile excitation the spectral shape of these graphs is similar to that of graph 2 and is taken into account by the normalization of the above calculations to the data. For the target excitation these graphs give rise to a continuous background which can be subtracted in the analysis.

In our experiment alpha-proton scattering has been measured at a beam momentum of 7 GeV/$c$ which is close to the maximum momentum for SATURNE. A liquid-hydrogen target of 4 cm thickness was used. Scattered $\alpha$ particles were momentum analyzed in the SPES IV magnetic spectrometer [13] and detected behind the focal plane by two drift chambers separated by 1 m. From the position of the particles in the six planes of the chambers the trajectories were calculated back to the target position. The time of flight between scintillators at the intermediate focus and the focal plane and the $\Delta E$ signals from four 1-cm-thick plastic scintillators were used for an unambiguous identification of the scattered $\alpha$ particles. The momentum acceptance of the spectrometer is 6%, so a complete spectrum was covered by four to five magnetic field settings. Missing-energy spectra ($\Omega = E_i - E_f$) were measured at four scattering angles of 0.8, 2.0, 3.2, and 4.1 degrees; the one obtained for 0.8° is shown in the upper part of Fig. 2. The spectrum indicates a strong rise of the yield above the $\pi$ threshold and a pronounced structure above 400 MeV. The part above the $\pi$ threshold has characteristics similar to the old data [10]. A calculation of graph 2, adjusted in the spectral height to the data above the $\pi$ threshold, gives rise to the solid line. The shape of the spectrum is quite well reproduced up to a value of $\Omega$ of 400 MeV. At larger values of $\Omega$ we observe a structure indicating a strong excitation of the $P_{11}$(1440 MeV) resonance. The difference spectrum—in which the projectile excitation is subtracted from the measured spectrum—is shown in the lower part of Fig. 2 which shows a pronounced peak in the $P_{11}$(1440 MeV) resonance region. Above 0.9 GeV the yield is rather flat. This is the region of the $D_{13}$(1520 MeV) and $S_{11}$(1535 MeV) resonances which can be excited in inelastic $\alpha$ scattering by $L=1$ transfer.

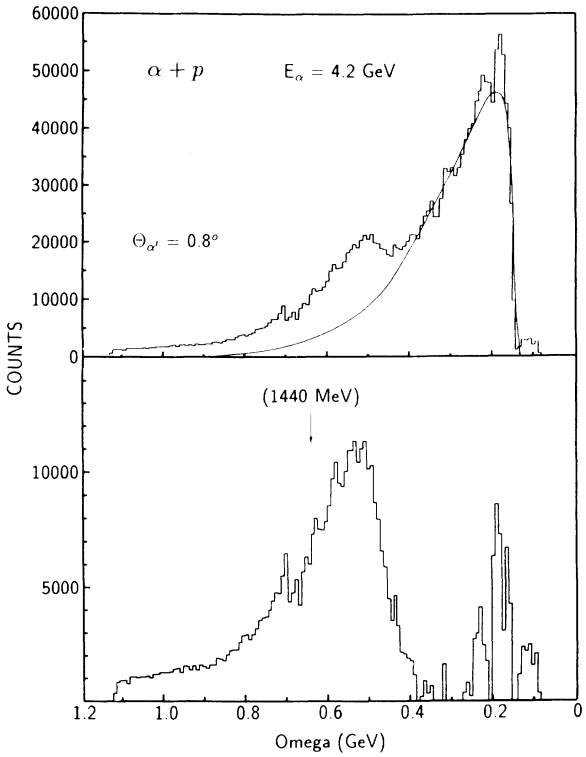


FIG. 2. Upper part: Missing-energy spectrum of inelastically scattered $\alpha$ particles on a hydrogen target. The solid line shows the spectral shape calculated for projectile excitation (graph 2 in Fig. 1) which was adjusted to the data above the $\pi$ threshold. Lower part: Difference spectrum between data and solid line.

The excitation strength in the lower part of Fig. 2 peaks at a value of $\Omega$ which corresponds to an excitation energy of 410–420 MeV with a width of about 120 MeV. As a result of the momentum-transfer dependence of the $\alpha$-particle form factor, which has to be taken into account, the strength is shifted to lower values of $\Omega$. To obtain the strength function, the form-factor dependence has to be unfolded. This is only known for small momentum transfers [14]; the extrapolation gives rise to uncertainties in the extracted resonance parameters. Our estimates give a shift of only 30–50 MeV in the peak energy and a 30–60 MeV increase in the resonance width, indicating a $P_{11}$ resonance at a mass of about 1400 MeV with

a width of about 160–170 MeV. The energy is rather low in comparison with the average energy from $\pi$-$N$ phase shift analyses [15]; the position corresponding to 1440 MeV (by including the effect of the $\alpha$ form factor) is indicated in Fig. 2.

Differential cross sections are given in Fig. 3. They show a very steep angular dependence characteristic of a monopole transition. Estimates using simple scaling assumptions of experimental monopole cross sections [16] indicate that the large cross sections obtained for the Roper resonance excitation imply a large fraction of the monopole sum-rule strength. The differential cross sections are quite well described in a folding-model approach including distorted wave effects [17]. The obtained differential cross sections (solid line in Fig. 3) are in good agreement with the data assuming a sum-rule strength of (70–80)%. Details of these calculations are discussed in a forthcoming paper.

Further support for a monopole character of the excitation results from the similarity of the data in the upper and lower parts of Fig. 3. Projectile excitation is dominated by the $\Delta$ resonance which also presents a monopole ($L=0$) excitation (however, of different spin-isospin structure). Therefore, the angular distributions should be similar for both cases. This is in fact true. A slightly flatter angular distribution for projectile excitation might be expected due to the three-body character of this reaction (dashed lines in Fig. 3).

From the centroid energy $E_x$ of the scalar monopole excitation the compressibility $K$ of a system may be deduced, where $K$ is defined for a spherical system with dimension $r$ by $K=r^2d^2(E/N)/dr^2$, corresponding to the curvature in the equation of state at the ground-state minimum. Using operator sum rules [18] for the nucleon this leads to

$$K_N=(m_N/3\hbar^2)E_x^2\langle r_N^2\rangle, \quad (1)$$

where $m_N$ is the nucleon mass and $\langle r_N^2\rangle$ relates to the mean-square radius of the scalar density.

In the constituent quark model the rms radius is directly related to the oscillator constant by the virial theorem giving rise to a nucleon radius which is far too small ($\langle r_N^2\rangle\sim 0.37$ fm$^2$). Therefore, for the understanding of the radial properties the inclusion of sea-quark polarization is important. The value of $\langle r_N^2\rangle$ is not well known. For electromagnetic coupling (dominated by the coupling to vector mesons) the rms radius is obtained from the proton and neutron charge-radius difference [19] which gives an isoscalar mean-square radius of about 0.62 fm$^2$. For the scalar density which couples to the $\sigma$ ($2\pi$ mode) the radius may be obtained from the analysis of the elastic $\alpha$-$p$ scattering which gives a square radius in the order of 0.6 fm$^2$. This yields a nucleon compressibility $K_N$ of $1.4\pm 0.3$ GeV. The errors are due to the uncertainties in the extraction of the excitation energy, the monopole matrix element, as well as the energy of the remaining monopole strength.

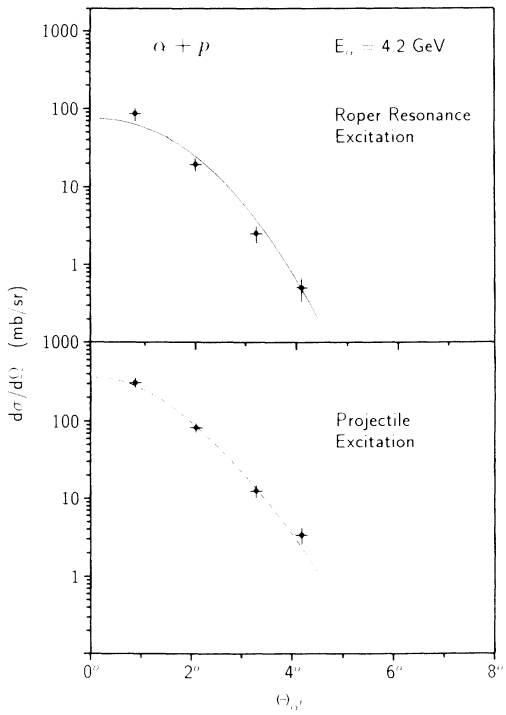


FIG. 3. Differential cross sections for excitation of the $P_{11}$ resonance excitation (upper part) and of the projectile (lower part). The errors given are mainly due to uncertainties in the separation of target and projectile excitation. For the $P_{11}$ excitation a triangular background from 0.35 to 0.9 GeV was subtracted. The solid line shows the calculated monopole cross sections obtained in a folding model. The angular distribution estimated for projectile excitation is shown by the dashed line.

Values of the compressibility can be derived from different models. For the constituent quark model a value of $K_N$ of 3 GeV is obtained using a harmonic oscillator with $\hbar\omega=500$ MeV. More complicated versions of this model as well as MIT bag estimates are discussed in Ref. [20] and give $K_N$ in the order of 900–1200 MeV.

In summary, a strong excitation of the Roper resonance has been observed in $\alpha$-proton scattering which demonstrates that this resonance represents the lowest compressional mode of the nucleon. Although consistent with other experiments, the energy of this $P_{11}$ resonance is somewhat lower than obtained from $\pi$-$N$ phase shifts. For the first time an experimental estimate of the compressibility of the nucleon has been obtained which lies between the values deduced from different models.

We would like to acknowledge active support from the SATURNE machine group and the cryogenic service during our experiment. One of the authors (H.P.M.) thanks the LNS for hospitality and interest in this work.

[a]Also at Institut für Kernphysik, Forschungszentrum

Jülich, D-5170 Jülich, Germany.
[b]Permanent address: Indiana University Cyclotron Facility, Bloomington, IN 47405.
[c]Permanent address: Soltan Institute for Nuclear Studies, Pl-00681 Warsaw, Poland.

[1] See, e.g., N. Isgur and G. Karl, Phys. Rev. D **18**, 4187 (1978); **19**, 2653 (1979); S. Capstick and N. Isgur, Phys. Rev. D **34**, 2809 (1986).
[2] F. Stancu and P. Stassart, Phys. Rev. D **41**, 916 (1990), and references therein.
[3] See, e.g., A. J. G. Hey and R. L. Kelly, Phys. Rep. **96**, 71 (1983); R. K. Bhaduri, *Models of the Nucleon* (Addison-Wesley, Reading, MA, 1988).
[4] See, e.g., G. Atkins, C. R. Nappi, and E. Witten, Nucl. Phys. **B228**, 552 (1983); G. Holzwarth and B. Schwesinger, Rep. Prog. Phys. **49**, 825 (1986).
[5] U. G. Meissner, N. Kaiser, and W. Weise, Nucl. Phys. **A466**, 685 (1988).
[6] G. E. Brown, J. W. Durso, and M. B. Johnson, Nucl. Phys. **A397**, 447 (1983).
[7] P. J. Mulders *et al.*, Phys. Rev. D **27**, 2708 (1983).
[8] P. A. M. Guichon, Phys. Lett. **164B**, 361 (1985).
[9] C. Hajduk and B. Schwesinger, Phys. Lett. **140B**, 172 (1984); A. Hayashi and G. Holzwarth, Phys. Lett. **140B**, 175 (1984).
[10] F. L. Fabbri *et al.*, Nucl. Phys. **A338**, 429 (1980).
[11] V. Dmitriev, O. Sushkov, and C. Gaarde, Nucl. Phys. **A459**, 503 (1986).
[12] R. Baldini-Celio *et al.*, Nucl. Phys. **B107**, 321 (1976).
[13] E. Grorud *et al.*, Nucl. Instrum. Methods Phys. Res. **188**, 549 (1981).
[14] J. Banaigs *et al.*, Nucl. Phys. **A445**, 737 (1985).
[15] Particle properties data booklet, Phys. Lett. B **239**, 1 (1990); for recent $\pi$-$N$ phase shift analysis, see R. E. Cutkosky and S. Wang, Phys. Rev. D **42**, 235 (1990).
[16] H. P. Morsch *et al.*, SATURNE Proposal No. 220, 1989.
[17] The folding-model calculations have been performed in the same way as discussed for the excitation of the giant monopole resonance in nuclear systems; see, e.g., H. P. Morsch *et al.*, Phys. Rev. C **22**, 489 (1980).
[18] Sum rules have been extensively discussed for nuclear excitation of the giant monopole resonance; see, e.g., O. Bohigas, A. M. Lane, and J. Martorell, Phys. Rep. **51**, 276 (1979); B. K. Jennings and A. D. Jackson, Phys. Rep. **66**, 143 (1980).
[19] R. W. Berard *et al.*, Phys. Lett. **47B**, 355 (1973).
[20] R. K. Bhaduri, J. Dey, and M. A. Preston, Phys. Lett. **136B**, 289 (1984).